THE MINISTRY OF NATIONAL INFRASTRUCTURES

GEOLOGICAL SURVEY OF ISRAEL

The effect of base level changes on the groundwater system between the Mediterranean and the Dead Sea base levels in Israel

Yechieli, Y., Kafri, U., Wollman, S., Shalev E. and Lyakhovsky, V.

Jerusalem, August 2009 **Report GSI/10/2009**

Abstract

The effects of base (sea or lake) level changes on the location and elevation of the groundwater divide were examined in the hydrological system between the Mediterranean Sea and the Dead Sea. Steady-state simulations were conducted with a 1-D analytical model and transient conditions were simulated using FEFLOW groundwater modeling software. Two hydrological scenarios were simulated: a) a transition to a new steady-state, following the expected drop of 150 m of the Dead Sea level; and b) the time of the precursor of the Dead Sea (Lisan Lake), some 20,000 years ago, when the lake level was about 250 m above the present-day Dead Sea level and the Mediterranean Sea level was 120 m below its present one. The results of the simulations show that the Dead Sea level drop has led to a progressive decline in the groundwater level up to several kilometers inland from the shoreline. The hydraulic gradient increases, and thus the discharge to the lake also increases at the expense of the storage, and also due to a small enlargement of the recharge zone by a ~600 m shift of the divide.

Broadly, the subsurface hydrologic system is compartmentalized into several sections, separated by low permeability fold structures bounding the mountainous uplands. Most of the groundwater recharge occurs in the uplands. Given this geometry and the available water level measurements, analytical and numerical modeling results show that only changes in the Dead Sea level and recharge rate result in dramatic changes for the scenarios examined. Limited by the low permeability folds, the effects of the Dead Sea level on the groundwater level are most pronounced in the vicinity of the Judea Desert lowland. The folds also greatly limit migration of the groundwater divide associated with changes in the Dead Sea level. Transient simulations show a peak increase of ~30% in the Dead Sea groundwater flux in ~75 years, resulting from drainage of lowland aquifers. After more than 500 years the groundwater flux is expected to return to values no more than 4% higher than at the beginning of the simulation. This small net increase is consistent with the small shift in the groundwater divide.

1. Introduction

The effect of base level changes and the structural configuration on their related groundwater systems in the world is very important, particularly where both marine and nearby inland base levels below sea level were subjected to considerable current and young changes still within the hydrological memory. In such cases, consequent shifts in groundwater divides , as well as in groundwater flow gradients, depend strongly on the structural configuration in between. Examples for systems where base levels (sea level) have changed in the recent past (20,000 years ago) are the Imperial Valley, California (e.g., Loetz et al., 1975, Kafri, 1984), the Afar depression, East Africa (e.g., Fouillac et al., 1989) and the Qattara depression, Egypt (e.g., Thiele et al., 1970). In most cases, this subject was dealt with regarding changes in coastal aquifers as a result of variations in sea level due to climate changes since the last glacial period (.e.g,, Essaid, 1990). Other studies attempted to simulate the possible effect of global warming and the consequent sea level rise on coastal groundwater systems (e.g., Sherif and Singh, 1999; Oude Essink, 2001; Tyagi, 2005). A few studies discussed the effect of changes in lake levels on their adjoining groundwater systems. Among the examples is that of Mono Lake (e.g., Rogers and Driess, 1995).

The main objective of this study is to examine the response of the groundwater divide to both natural and man-made changes in the elevation of the base levels. This was studied in the groundwater system between the Mediterranean and the Dead Sea (DS) base levels. This system represents an example which underwent, and is still subject to, considerable base level changes, and is strongly controlled by the structural configuration. The effect of the geological structure on the water divide was elaborated on by simulations that assessed future and past groundwater levels, the discharge to the lake, as well as the location of the groundwater divide.

2. Hydrogeological background

The main geological structure in the study area is the anticlinorium of the Judea and Samaria mountains (Fig. 1), which by itself consists of a few NE-SW trending anticlines. The anticlinorium dips to the coastal plain of Israel. The same configuration prevails in the east where the structure dips in an undulating form toward the DS Rift. The western (Ramallah) monocline is underlain by a reverse fault, and its influence on the hydraulic conductivity and flow gradient has been analyzed previously (Yechieli et al., 2007).

The Judea Group Aquifer (JGA) discussed herein, which consists mainly of Cretaceous carbonate rocks, is the largest active aquifer in Israel. This aquifer, some 600-700 m thick, is recharged along the Judea and Samaria mountain crests of central Israel. It dips to the west towards the Mediterranean coastal plain and to the east toward the Jordan River-DS valley. On both sides, the aquifer is confined under a thick sequence of Upper Cretaceous and younger layers . At the bottom, it is confined by Lower Cretaceous layers (Qatana Fm.) (Fig. 1b). To the west, close to the Mediterranean coast, the JGA carbonate sequence passes laterally into the Talme Yafe Formation, of low permeability. This configuration, exhibited on a W-E directed cross-section between the Mediterranean Sea and the Dead Sea Rift (Fig. 1b), assumingly does not enable hydraulic connection of the aquifer to the sea and blocks seawater intrusion into the aquifer.

The aquifer is replenished along the mountain crests where a groundwater divide is formed between the western and eastern drainage basins. The groundwater flows from the recharge zone to the Mediterranean coastal plain in the western portion of the aquifer. Due to the overlying confining layers and the assumed blockage of flow to the west by the Talme Yafe aquiclude, the aquifer has apparently no connection to the sea. Thus, most of its past natural drainage was through the large Yarqon and Taninim springs and at present most is pumped through water supply wells and the rest is through the Taninim spring, north of the study area (Fig. 1a).

To the east, groundwater flows toward the Dead Sea Rift (DSR) base level. Parts of the flow emerge along the flow path as springs. Most of the flow down-gradient seems to be blocked along the Rift margins by the impervious graben fill and as a result emerges in several specific locations, which are also structurally controlled, through the large springs of Zuqim, Qane and Samar (e.g., Guttman, 1998a; Laronne and Gvirtzman, 2005).

The groundwater system in Israel is, at present as well as in the past, controlled by two base levels, namely the Mediterranean in the west and the DSR in the east. The present configuration of the water divide between these two systems was studied by Matmon (1995). During the young geological history, still within the hydrological "memory", both base levels underwent drastic changes which affected their adjoining groundwater systems. The Dead Sea level is presently declining at the rate of 1 m/year, a process that began in the 1960's because of the negative water balance of the DS, due to the extraction of water from the north (by Israel, Jordan and Syria) and pumping of the DS brine by the Dead Sea Industries (e.g., Lensky et al., 2005). This decline, in turn, results in a drop in the groundwater levels in the adjoining groundwater system (Kafri and Arad, 1978; Kafri, 1982: Yechieli, 2006; Yechieli et al., 1995). Another result of the drop in the DS levels was suggested to be an increase in groundwater flow toward the DS (Salameh and El-Naser, 1999). In addition, the above-described combined process is responsible for the ongoing process of sinkhole formation along the DS coastal plain (Abelson et al., 2006).

The JGA is subdivided into a lower and an upper part (Fig. 2). The lower JGA consists mostly of bedded, fine crystalline, somewhat chalky dolomite and limestone. The upper JGA contains more coarse crystalline and sometimes reefal limestone and dolomite, interbedded with chalky limestone and chalk. In the upper JGA, karst phenomena such as solution channels, caves and open cracks are more abundant as compared to the lower JGA. Thus, the upper JGA seems to exhibit a hydrologically more conductive sequence than the lower JGA.

In some previous studies by, e.g., Guttman (1980, 1998), Guttman and Rosenthal (1991), the JGA in the study area was separated into lower and upper aquifers or sub-aquifers. However, they pointed out that the two sub-aquifers in the eastern portion of the study area are connected (Guttman and Rosenthal, 1991). The identical water levels in the Yericho 4 and 5 boreholes in both sub-aquifers support the connection between the two sub-aquifers. Thus, the JGA is regarded in the present study as one hydrological unit, exhibiting somewhat different hydrological properties in its lower and upper portions.

The groundwater of the JGA in the recharge zone and somewhat down-gradient is fresh, with concentrations between a few tens to several hundreds mg/l Cl. To the east of the recharge zone, salinities in the upper aquifer are low. Fresh water in the upper part of the JGA exists even close to the DSR base level. In the lower part of the JGA and close to the DSR base level, salinities varying between several hundred to over 10,000 mg/l Cl are attributed to either mixtures of fresh waters with present day DS brine or with older trapped brines. Here, the interface or interfaces (in the case of a multi-system) are detected, both hydrologically and geophysically, between the fresh water and the underlying brine bodies (Kafri et al.1997;

Yechieli et al., 2001; Kiro et al., 2008). The interface between the fresh groundwater and the DS brine (present Cl concentration of ~220,000 mg/l) is shallow and of moderate slope due to the large density difference between the fresh water and the brine (Yechieli, 2000).

3. The basic inputs for the model

The observations and assumptions which dictated the inputs to the model are as follows:

3.1 Rainfall and recharge

Average yearly rainfall values are constrained based on the data from the Israel Meteorological Service. In most of the recharge zone, the rainfall is around 650 mm/yr (Fig. 2). These values drop sharply to 400 mm/yr in the eastern margins of the recharge zone and farther east to less than 100 mm/yr near the DS. In the western part of the section, there is no direct recharge to the aquifer since it is covered by a thick confining sequence. In the central recharge zone, analogous to other regions of similar hydro-meteorological situations, recharge ratios can attain a value of up to 50% of the total precipitation (e.g., Kafri and Kessler, 2001). In the present study, a more conservative value of 40% recharge is used. Following Guttman (1998), the recharge ratio in the eastern recharge zone is some 30% of the precipitation. In the Judea Desert, more to the east, most of the area does not allow direct recharge. In the limited areas of the Judea Desert where the JGA is exposed, due to the very low precipitation, recharge seems to be very small and, for all practical purposes, negligible.

3.2 Groundwater levels and flow gradients

Water-level data along the cross-section studied are sparse and not synchronous. Nevertheless, the obtained general configuration of the water table reflects the geological structure. In the central recharge zone of the Jerusalem region water levels are between 450-480 m above sea level (asl) and the divide is located close to the En Karem 3 borehole (Fig. 1b). Flow gradients are small, around 0.2%. In the eastern watershed, from the divide eastward, the gradient (interpolated between the En Karem 3 and Jerusalem 5 boreholes) is already steeper, around 1.5%. Farther to the east (between the Jerusalem 5 and Mitzpe Yericho 2 boreholes, Fig. 1) the gradient increases to 5%. Towards the DS, the gradient is again small, around 0.6%. In the western watershed, from the divide westward, the flow gradient (interpolated between the En Karem 3 and Eshtaol 2a boreholes) is steep, around 5%. It is assumed that in this particular portion of the section, the 5% gradient is an average of a steeper gradient in the flexure zone, as discussed by Yechieli et al. (2007). From the foothill region westward to the coastal plain, the gradient is extremely small, less than 0.1%.

3.3 Estimation of hydrological parameters - transmissivities (T) and conductivities (K)

Hydrological parameters along the cross-section and its vicinity are relatively sparse and variable. Some were obtained from pumping tests (Table 1) and some from previously calibrated models. It is assumed that the K values are somewhat higher in the upper sub-aquifer due to its geological features (e.g., karst, reefal limestone).

An attempt was made to find the general relationship between the structural positions and their respective K values, obtained from pumping tests. The a-priori assumption was that anticlinal structures are prone to develop a more intense open fracture network and as a result, exhibit higher K values as compared to less fractured synclines with lower values. The K values exhibit a reasonable correlation with the thickness of the overlying Mt. Scopus Group sequence, which reflects the structural position (Fig. 3). Thus, in general, the higher K values characterize elevated structures and the lower ones characterize the synclines, in both sub-aquifers.

Accounting for the general geological structure, the model cross-section was subdivided into five segments according to their K values. The main segments are: the central recharge zone, the western coastal plain and foothills, the western structural flexure zone, the eastern flexure and the Judea Desert (Fig. 2). The main segments were subdivided, in addition, based on structural considerations and existing hydrogeological data. The following is a description of the main segments, based on field data, on previous simulations and on the best estimates from calibration in the current simulations.

3.3.1 The central recharge zone of the Judea Mountains

This segment of the model is characterized by the fact that only the lower, less conductive, part of the JGA is saturated and the upper portion is in the vadose zone. T values obtained from pumping tests are variable. Locally, low (10^1 m^2/d) and high (10^3 m^2/d) T values were found. The respective calculated K values are 10^{-2} m/d and 10^1m/d. A common T value of 10^2 m^2/d was also employed in previous models (Guttman, 1998; Berger, 1999). The saturated thickness is mostly around 200 m and, in places in the SE of this area, up to 480 m. K values are thus commonly around 1 m/d and the model was calibrated accordingly (calibrated values of 1.3-2.6).

3.3.2 The western coastal plain and foothills

In this segment of the model, which crosses synclines and structural highs (Fig. 2), the entire JGA is saturated and thus the upper more conductive portion of the aquifer is incorporated in the system. T values, obtained from pumping tests (Guttman, 1998) and calibrated models (e.g., Berger, 1999), were found to be up to 10^4 m^2/d. The T values of both (connected) parts of the JGA vary between 10^1 and 10^4 m^2/d (Guttman, 1998) and the respective calculated K values are between 1 and 10^2 m/d (calibrated values of 1-30 m/d).

3.3.3 The western flexure zone

This segment of the model represents a steep flexure zone, with an average 15^0 dip. Locally, within the flexure zone, dips can be as high as 50^0. The groundwater flow gradient from the recharge zone through this flexure zone becomes very steep, indicating reduced K values. These reduced K values in the western flexure zone are due to compression induced by the folding of the anticline (Yechieli et al., 2007).

T and K values along the western flexure zone exhibit in fact a wide range of values between 10^2 - 10^4 m^2/d and 10^{-1} – 10^1 m/d (Table 1). Very low K values were designated accordingly in order to satisfy the steep gradient configuration (calibrated values of 0.1-0.2 m/d).

3.3.4 The eastern flexure zone

Similarly to the western flexure, low T values (~ 4 and 15 m^2/d) were designated in the eastern, although milder, flexure in a model by Guttman (1998). Low K values were also designated accordingly herein (calibrated values of 0.3-0.6 m/d).

3.3.5 The eastern Judea Desert

This segment of the model consists of synclines and anticlines. In the structurally elevated areas, only the lower part of the JGA is saturated; and in the synclines, also portion of the upper part is saturated. The overall T values are, therefore, expected to be smaller than in the west. Kronfeld et al. (1990) claimed, based on a natural isotope study, that flows in the lower JGA in this area are slower compared to those in the upper JGA, which is in agreement with the lower K values claimed here for that part of the JGA. T values from pumping tests are rare, varying between 10^2 and 10^4 m^2/d, and respective calculated K values are between 10^{-1} and 10^1 m/d. The above values seem to reflect different structural configurations as well as variable specific local conditions. Accordingly, higher K values in the model were assigned to the structural elevated areas and smaller ones to the synclines, namely calibrated values of 0.3-8 m/d.

4. Analytical and numerical modeling

The hydrogeological system between the base levels of the Dead Sea and the Mediterranean Sea was examined by both analytical and numerical simulations. The first stage employed the analytical approach in order to test the principle effects of a geological structure. The second stage used the numerical simulations in which the specific hydrogeological conditions of the present configuration were considered.

4.1 Examination of the effect of the geological structure on the location of the groundwater divide – an analytical approach

The geological structure was a-priori assumed to have a significant effect on the location of the water divide. Thus, the effect of the Judea and Samaria anticlinorium on the location of the groundwater divide due to variations in the elevation of the base levels on both sides was examined. This structural effect could be manifested in the distribution of the permeability field (Yechieli et al., 2007), in the location of the recharge zone and in the geometry of the base of the aquifer. Numerical and analytical simulations were run in order to examine separately the effect of each of the above factors on the location of the divide in general and specifically in the cases of a change in the level of the base levels.

An analytical solution is presented here for the hydraulic head distribution in a heterogeneous aquifer which is divided into several homogeneous segments (Fig. 4). Assuming the Dupuit approximation, the two-dimensional equation for steady-state flow in a homogeneous aquifer could be reduced to a one-dimensional equation for a hydraulic head, *h* (Bear, 1972):

$$T\frac{\partial^2 h}{\partial x^2} + \mathrm{R} = 0 \tag{1}$$

where the transmissivity is T=KB, K is the hydraulic conductivity, B is the thickness of the saturated part of the aquifer, and R is recharge from rain. This approximation assumes that the thickness of the saturated part of the aquifer is considerably larger than the hydraulic head variations.

For a constant recharge the solution for equation (1) is:

$$h(x) = -\frac{\mathrm{R}}{2T}x^2 + bx + c \tag{2}$$

This solution can be extended for a heterogeneous aquifer which is by itself divided into several homogeneous segments. For each segment, *i*, with recharge R_i, and transmissivity T_i the solution for h_i is:

$$h_\mathrm{i}(x) = -\frac{\mathrm{R_i}}{2T_\mathrm{i}}x^2 + b_\mathrm{i}x + c_\mathrm{i} \tag{3}$$

where b_i, c_i, are the integration coefficients. The boundary conditions are given at the left (x=0) and right (x=L) edges of the aquifer. The aquifer is divided here into five segments and the hydraulic heads are prescribed at the boundaries:

$$\begin{aligned} \mathrm{h}\big|_{\mathrm{x=0}} &= \mathrm{h}_1 \\ \mathrm{h}\big|_{\mathrm{x=L}} &= \mathrm{h}6 \end{aligned} \tag{4}$$

At the connection of segments *i* and *i*+1, two conditions are defined,

continuity of the hydraulic head:

$$-\frac{\mathrm{R}_i}{2T_i}L_i^2 + b_iL_i + c_i = -\frac{\mathrm{R}_{i+1}}{2T_{i+1}}L_i^2 + b_{i+1}L_i + c_{i+1} \tag{5}$$

and continuity of flux:

$$T_i\left(-\frac{\mathrm{R}_i}{T_i}L_i + b_i\right) = T_{i+1}\left(-\frac{\mathrm{R}_{i+1}}{T_{i+1}}L_i + b_{i+1}\right) \tag{6}$$

For the five segments and four segment connections, equations 5 and 6 are repeated four times for i=2, 3, 4, 5. Eight equations are written for the segment connections together with two boundary conditions (eq. 4) yielding a system of ten linear equations for ten unknown b_i and c_i (i=1-5). This set of equations is solved numerically and $h(x)$ is calculated using equation (3) for given recharge and transmissivity values.

The above analytical solution allows examining the effect of different factors on the groundwater table configuration and location of the water divide between both base levels (Fig. 4). Figure 4a shows the effect of the distribution of recharge along the traverse with a uniform T of 1,000m^2/day. In the simplest case of the uniform recharge, the water head is parabolic with the maximum (water divide) in the center of the profile. The solution for the case with the limited recharge zone in the central part of the traverse, reflecting the current actual situation discussed above, is parabolic only within the rechargeable segment and linear outside this segment. A slight asymmetric location of the middle segment leads to a small westward shift of the divide location. In the hypothetical case of recharge confined to the western part, the divide is significantly shifted to the west (Fig. 4a).

In the case of a uniform T, the location and the elevation of the groundwater divide is considerably changed due to changes in elevation of the base levels (Fig. 4b). The case with the equal base levels (Fig 4a) corresponds to the initial Pliocene time configuration. The hydrological situation during the Late Pleistocene was a low Mediterranean Sea level of about -120 m and a relatively high Lisan Lake level of about -180 m (Fig. 4b). The present Mediterranean and DS levels (0 m and -395 m, respectively) and the predicted Mediterranean and DS levels (0 m and -545 m, respectively) yield different results (Fig. 4b). The decline of the DS level leads to a significant drop of the water table westward and a shift of the water divide. The water divide drops to below zero and in the extreme case of the low standing DS, enables continuous flow of water from the Mediterranean to the Dead Sea. This case is highly hypothetical, since the T values are not expected to be uniform due to the effect of the structure, as schematically presented in Figure 4c. The T differentiation reflects the existence of a structure and some actual values of the five segments. The solution for the present levels (0, -395m) fits the measured water-head values quite well (Fig. 4c). For the cases of the Lisan Lake and the future DS (Fig. 4c), the variations in the elevation of the base levels cause only a slight change in the location of the groundwater divide. The main conclusion from the above simulations is that all hypothetical possibilities of a non existing structure yield groundwater configurations which do not agree with the one actually observed . An existing structure seems to be, thus, the major controlling factor on the groundwater table configuration.

While the above analytical approach can examine quite well some of the effects of the structure on the water divide, a specific hydrogeological situation can only be described by a 2-D numerical modeling. Following are the expected general differences between the analytical and numerical modeling of the case studied: The analytical solution keeps constant T-values in spite of changes of the aquifer thickness (B-value). Hence, this solution probably overestimates change in the water level following the drop of the base level. Combining the base level change, the thickness of the phreatic aquifer and the flow pattern requires a 2-D numerical modeling, which is presented in the following section. The separation of the aquifer into two sub-aquifers could not be simulated with the 1-D approach. Moreover, the 1-D simulation could not consider the effect of anisotropy. The effect of the geometry of the base of the aquifer could not be examined with the 1-D analytical simulation.

Due to the limitation of the 1-D analytical simulation in the present study, another set of simulations was conducted with the 2-D FEFLOW numerical modeling. One of the main differences is that the analytical approach could not simulate a transient scenario which was necessary for the calculation of the change with time in discharge to the Dead Sea. The effect of density-driven flow could not be simulated with the 1-D simulation and thus the location of the fresh-saline water interface could only be determined with the 2-D code. The results of the above analytical solution are good enough because the saline water body is found only in a small portion of the model domain.

4.2. The 2-D FEFLOW code

4.2.1 Model configuration

The 2-D model coincides roughly with a W-E directed geological cross-section between the Mediterranean and the DSR (Fig.1). The cross-section is perpendicular to the hydrological equi-potential lines and it crosses near the few existing boreholes which yield available relevant hydrogeological information for calibrating the model. The flow occurs in the Judea

Group Aquifer (JGA), whose total thickness is taken as 700 m, the most frequent value, where no direct information is available.

The lower boundary of the model is the impermeable confining layers of the Qatana Marl (Fig. 1). The structural configuration of this boundary is based on the 1:50,000 structural map (Fleischer and Gafsu, 1998). The upper boundary is the ground surface. The western boundary is in the coastal plain. The eastern boundary is the DS base level and the graben fill sequence.

The first step of the present study was to calibrate a 2-D E-W hydrogeological model between the two base levels of the Judea Group aquifer, namely the Mediterranean Sea in the west and the DSR in the east (Fig. 1). Satisfactory calibration consequently enabled simulation of both the palaeohydrological configuration at the time of the last glacial period (end of the Lisan Lake) and the future configuration related to the ongoing decline of the DS base level.

Since the purpose of the present work was only to get a rough estimate of the effect of the DS level changes on the groundwater system, the spatial variations in the north-south direction were ignored, and a representative east-west 2-D cross section was used. This is, of course, a potential limitation to the model. The intention in the future is to simulate the situation again in 3-D simulations, taking into consideration the geological structures whose axes are oblique to the flow direction obtained from the simulation of the 2-D cross-section. This can be done provided that more data becomes available regarding the spatial distribution of permeabilities and water levels.

The FEFLOW numerical code (Diersch, 2005) was used for the 2-D groundwater model simulation. Variable density flow was used to account for the DS brine/fresh water interface (hereafter DS interface). The 2-D model was calibrated under steady-state conditions as of the year 1960 in order to obtain values of hydraulic conductivity (Fig. 2). The 1960 DS level was preceded by a 20 year, approximately constant level, and was considered an approximately steady-state situation. The steady-state boundary conditions were set as follows:

- The western boundary – This boundary was set in the coastal plain region, at a distance of some 10 kilometers east of the Mediterranean shoreline, or at the Talme Yafe Formation. The assumption here was that the aquifer is blocked to the sea but still drains northward to the

Taninim spring (Fig. 1). Therefore, a specified head of +10 m and zero salinity were attributed to this point. Hence the head boundary is related to the sea although there is no simple hydraulic connection between the sea and the aquifer.

- The eastern boundary (Dead Sea) – specified the DS level at 395 m below sea level (bsl) with the specified head adjusted for DS brine density of 1.23 g/cm^3 and salinity of 340,000 mg/l.
- The upper boundary - Recharge zone – specified vertical influx of 7.12×10^{-4} m/d (0.26 m/yr) for the central recharge zone and 3.56×10^{-4} m/d (0.13 m/yr) for the eastern recharge zone, yielding a total recharge of 4.9 mcm/yr per strip of 1 km-width where mcm is a million cubic meters.
- The lower boundary – the impervious Qatana Formation of insignificant leakage.

A finite element mesh was constructed with approximately 9000 triangular elements. A higher density of mesh elements was used in the DS interface zone and in the western flexure zone in order to allow for a better resolution in these complicated areas.

Two general vertical zones of hydraulic conductivity were established to represent the assumed K difference between the upper and lower JGA sequence. Further lateral sub-divisions of these zones were based on transmissivity values obtained from aquifer test results as well as on structural considerations (discussed above). The value of the anisotropy ratio between maximal and minimal K was set at 10 - 100. A value of effective porosity of 0.07 (Kafri and Goldman, 2005) was used for the entire JGA sequence, and a value of 0.20 was used for the DS coastal plain graben fill, whose horizontal hydraulic conductivity was set as 20 m/d. The dispersivity values were 100 m in the longitudinal direction and 10 m in the transverse (vertical) direction.

The values of horizontal hydraulic conductivity were adjusted to enable matching the computed water levels as close as possible to the measured levels at the six boreholes along the model. The resulting steady-state water levels and the position of the DS interface are shown below. The computed steady-state groundwater flows to the DS and to the Mediterranean base levels are 2.6 and 2.3 mcm/yr/km-width, respectively (Table 2). The simulated groundwater divide is located very close to the En Karem 3 borehole.

4.2.2 Sensitivity analysis and examination of the effect of the lower boundary geometry

The calibration of the model yielded a fair agreement between the results obtained in the simulations and the actual water-level data. Sensitivity analyses were conducted to examine some of the factors that were used in these simulations (Fig. 5). These include the role of the lower boundary of the aquifer and its geometry and the distribution of the different conductivity values along the cross section.

The effect of the geometry of the lower impermeable boundary was examined by comparing the results of the previously run simulation, that used a structurally controlled impermeable boundary, with those of the new simulation that did not use such impermeable layer at the bottom. In the latter case, the lower no-flow boundary is 1000 m below the previous case and thus the geometry effect is insignificant. The latter simulations show lower water levels by about 500 m than the previously calibrated case with the impermeable layer, which fits the measured water levels. The uniform K case yields a result similar to the one obtained by the analytical analysis for uniform T (Fig. 5a). These simulations show that the geological structure, namely the geometry of the impermeable layer at the bottom of the aquifer, determines the actual water level distribution. The effect of variations in K values on the water level was found to be significant. For example, when K values of only the central recharge zone are reduced to half, the water level rises significantly by some 60 m.

The effect of variations in K values (Fig. 5b) – When K values of only the central recharge zone are reduced to half, the water levels rises significantly by ~60 m. When K values in this zone are doubled only a small decrease in water level of the divide (few meters) is evident. This can be explained by the fact that the water level in both flexure zones, east and west of the central recharge zone, are constant in this simulations and determined only by the values of flux and hydraulic conductivity. Therefore, an increase in K can not change significantly the shape of the hydraulic gradient which is quite shallow as exhibited in the previous calibrated run. On the other hand, a decrease in K can elevate significantly the water level due to the piling effect. In both cases, no significant change is observed in the western and eastern sectors of the section. A decrease in the K values of the flexure zone (Fig. 5b) affects significantly the water level pattern in both the flexures and the central recharge zones but not in the eastern and western zones. These simulations show that they are quite sensitive to changes in the K values, especially in the central recharge zone.

5. Simulations of past and future scenarios related to base level changes – results and discussion

Following the calibration of the model to the current situation, two scenarios are simulated as follows: the future scenario related to the expected continuous decline of the DS level and the past scenario at the peak of the last glacial period represented by high levels of the Lisan Lake.

5. 1 Simulations of the future DS decline scenario

The DS base (lake) level declined in the last fifty years at a rate of about 0.5 m/y and recently at the rate of 1 m/y. It will assumingly reach a steady state following a drop of approximately 150 m (Yechieli et al., 1998). A future stepwise simulation of the DS level decline assumes no significant future change of the Mediterranean base level. In the first simulation, the salinity and density of the DS brine is assumed to be constant. At a later stage, a simulation was conducted with a higher density (1.3 g/cc) and salinity (400 g/l), as expected in the future for the DS following considerable evaporation (Fig. 6). Rainfall and recharge in the recharge zone were assumed to be similar to the present-day amounts. The structural configuration, as well as the hydraulic conductivities (K), will supposedly remain constant.

A transient simulation was performed for the future declining DS level, using the 1960 year DS level (-395 m) as the initial condition with the present-day recharge flux. The estimated rate of decline of the DS level is shown in Figure 7, as predicted by Yechieli et al. (1998). The rate of the level decline is expected to decrease gradually to zero after 350 years, dropping to an elevation of -545 m . It is assumed herein that thereafter the DS will remain constant at that level.

The transient simulation was run for a period of 1000 years. The groundwater level and the position of the DS interface from the beginning and the end of the simulation are shown in Figure 6. The decline of the groundwater levels is primarily recognized in the eastern part of the aquifer close to the DS, with insignificant water-level changes near the groundwater divide. The change in the location of the groundwater divide at the end of the 1000 year simulation is rather small, namely, a westward shift of about 600 m (Fig. 8).

The change in the simulated groundwater flow rates to the DS is shown in Figure 7. The increase in flow, during the drop of ~1m/yr of the DS levels, is from an initial steady-state value of 2.6 mcm/yr/km-width in 1960 to a maximum of about 3.3 mcm/yr/km-width after 100 years. This increase is considered to be mostly due to steepening of the hydraulic gradient and release of storage. At the maximum flow values, the increase in flow is about 0.7 mcm/yr/km-width. The change in the drop rate of the DS levels after about 100 years (Fig. 7) causes a change in the trend of discharge to the DS. The flow to the DS decreases until it reaches a new equilibrium at about 2.7 mcm/yr/km-width after approximately 500 years, namely an additional 0.1 to the original 2.6 mcm/yr/km-width. This relatively small difference corresponds to the 600 m westward shift of the groundwater divide and the capture of some additional flow to the east.

The above calculated increase of flow to the DS along a 1 km wide strip cannot be simply extrapolated to the entire 50 km length of the western shore of the DS. This is mainly because part of the flow might be oblique and not parallel to the W-E trending longitudinal model section applied in this study, due to the complexity of the NE trending synclines and anticlines. Moreover, the present study does not include the eastern (Jordanian) drainage basin of the DS. A rough estimate yields an increase of less than 25% of the groundwater flow to the DS, which is far below the values calculated for the DS by Salameh and El-Naser (1999). The increase in flow is probably reduced by additional groundwater exploitation in the drainage basins on both sides of the DS.

The predicted change in the position of the DS brine/fresh water interface due to the decline of the sea level is shown by a dotted line representing the TDS of 170,000 mg/l, which is 50% of the DS brine salinity (Fig. 6). The obtained eastward shift of the interface is approximately 2 km. The simulation described of a higher brine density yields a fresh-saline water interface of a milder slope, as expected.

5.2 Simulation of the peak of the last glacial period scenario

Some 20,000 years ago, the configurations of both base levels were considerably different. The Mediterranean level was at 120 m bsl and that of the eastern Lisan Lake level, at approximately -180 m bsl. Salinity of the Mediterranean Sea at that time was not considerably different from the present level. The salinity of the Lisan lake was half that of the present DS brine (Katz et al., 1977; Begin, 2002) and water density was also lower. The structural configuration and the K values were the same as at present.

There is a certain dispute concerning rainfall and recharge in the recharge zone. During the time span discussed, average temperatures were assumed to be 10^0 C cooler than at present (McGarry et al., 2004). At that time, C-4 type temperate grass vegetation prevailed and the rainfall was claimed to be lower, around 250-300 mm/y (Bar-Matthews and Ayalon, 2003). On the other hand, Enzel et al. (2003) showed a relationship between the DS levels and rainfall, and claimed by extrapolation that the highest Lisan lake level is indicative of higher average rainfalls than the present one. Despite the above differences, the combination of a lower rainfall and lower evapotranspiration can yield a net recharge similar to that of a higher rainfall and higher evapo-transpiration. Because of the dispute and the unknowns described, the sensitivity of the above two possible scenarios, namely higher and present day rainfall and recharge, were examined.

Steady-state model simulations were run with the following boundary conditions:

- The western boundary – specified head of 120 m bsl and zero salinity.
- The eastern boundary (Dead Sea) – specified lake level at 180 m bsl with specified head adjusted for brine density of 1.115 g/cm^3 and TDS of 170,000 mg/l, which is half of the present-day density and concentration.
- The recharge flux (two scenarios) –100% and 150% of present-day flux, representing the assumed possible values.

The simulated steady-state water levels and flow rates are shown in Figure 9 and Table 2. For the 100% recharge case, the steady-state flow to the DS is about 2.5 mcm/yr/km-width, namely some 0.1 mcm/yr/km-width less than that of the present-day case (Table 2). This is explained by the 400 m eastward shift of the groundwater divide as compared to its present-day location. The 150% recharge case exhibits a steady-state flow to the Dead Sea of 1.1 mcm/yr/km-width greater than that of the present day. In this case, the divide is expected to be in the same location and somewhat higher, and the flow to the Dead Sea and the Mediterranean Sea are similar.

The position of the DS brine-freshwater interface for the two recharge scenarios is shown in Figure 9 as dotted lines representing 50% of the Lisan Lake solute concentration (85,000 mg/l). As expected, the location of the interface is 2-3 km west of the present-day interface, due to the higher elevation of the lake level during the last glacial period. The two different configurations of the interface correspond to the two recharge scenarios, whereby the most eastward location corresponds to the larger recharge (150%) scenario. The interface is steeper for the case of the Lisan Lake and shallower for the future DS situation, as expected, due to the difference in the density of the saline lake water of these two cases.

6. Summary and conclusions

The effects of base level changes on related groundwater systems between both base levels in the Mediterranean-Dead Sea system, were studied. The changes studied can assist in the assessment of similar past processes that prevailed or still prevail elsewhere in the world. The current rate of drop in the Dead Sea level is about 1 m/year. Regional scale simulations, from the Dead Sea across the water divide in the Judea Mountains to the Mediterranean base level, were conducted using the FEFLOW modeling code and an analytical solution.

Simulations were conducted for both future and past scenarios as follows: (1) 200-400 years from now, when the predicted continuous drop of the DS level will supposedly attain a new steady state about 150 m below the present one (2) the Lisan Lake period, some 20,000 years ago with lake level at 180 bsl.

The results obtained are as follows: 1) In the first scenario, a progressive decline of groundwater level is encountered to several kilometers inland from the DS shoreline. The eastern hydraulic gradient increases due to the significant drop in the Dead Sea level. As a result, the discharge to the DS is also expected to increase, at the expense of the storage. A small westward shift of the divide of several hundred meters is also expected. 2) In the second scenario, a rise in the groundwater level is observed in the simulations. Depending on the amount of recharge, the flow to the Dead Sea might increase. An eastward shift of the divide of about 400 m is also expected.

The geological structure was found to be a significant factor controlling the location of the groundwater divide. This structural effect is manifested in the permeability distribution, the location of the recharge zone and the geometry of the base of the aquifer. A drop of the base level has no considerable effect on the location of the divide in cases where there is a distinct anticline between both base levels, whereas without this structure the water divide is expected to shift several kilometers westward.

A comparison between the 1-D and 2-D simulations and the actual data shows that in many cases the analytical analysis yields good results. The 2-D simulations are necessary for the transient case where an estimate of the change with time is required (e.g., discharge to the sea). The 2-D simulations are also important for the determination of the location of the fresh-saline water interface.

Acknowledgements

We thank B. Cohen, H. Netzer and N. Almog for their assistance in the graphics. This study was supported by a grant from the Israeli Science Foundation 479/03. We also thank the anonymous reviewers whose comments helped in improving this article.

References

Abelson, M., Yechieli, Y., Crouvi, O., Baer, G., Wachs, D., Bein, A., Shtivelman, V., 2006. Evolution of the Dead Sea sinkholes In: Enzel, Y, Agnon, A., Stein, M. (eds.), New Frontiers in Dead Sea Paleoenvironmental Research, , Geol. Soc. Am., Spec. Paper, pp. 241-253.

Bar-Matthews, M., Ayalon,A., 2003. Climatic conditions in the eastern Mediterranean during the last Glacial (60-10 ky) and their relations to the upper Palaeolithic in the Levant as inferred from oxygen and carbon isotope systematics of cave deposits. In: Gorring-Morris, N. and Belfer-Cohen, A (eds.), More than Meets the Eye. Studies on Upper Paleolithic Diversity in the Near East, pp. 13-18.

Bear, J., 1972. Dynamics of Fluids in Porous Media. American Elsevier, New York.

Begin, Z.B., 2002. Computer simulation of salinity in the Late Quaternary Lake Lisan. Isr. J. Earth Sci. 51, 225-232.

Berger, D., 1999. Hydrological model of the Yarqon-Taninim aquifer (Yartan). Mekorot Water Co. (in Hebrew).

Diersch, H.-J., 2005. Finite element subsurface flow and transport simulation system, user's manual, FEFLOW version 5.2. WASY Gmb H. Berlin.

Enzel, Y., Bookman(Ken Tor), R., Sharon, D., Gvirtzman, H. ,Dayan, U. ,Ziv, B., Stein, M., 2003. Late Holocene climates of the Near East deduced from Dead Sea level variations and modern regional winter rainfall. Quat. Res. 60, 263-273.

Essaid, H.I., 1990. A multilayered sharp interface model of coupled freshwater and saltwater flow in coastal systems: Model development and application. Water Res. Res 26(7), 1431-1454.

Fleischer, L., Gafsu, R., 1998. Top Judea Group -Digital structural map of Israel. Phase II-Central Israel. Geophys. Inst. Rep. 873/55/99.

Foilacet, A.M., Foilacet, C., Cesbron, F., Pillard, F. and Legendre, O., 1989. Water-rock interaction between basalt and high-salinity fluids in the Asal Rift, Republic of Djibouti. Chem. Geol. 76, 271-289.

Guttman, J., 1980. Study of uranium isotopes in the Cenomanian-Turonian aquifer in the Yarqon-Taninim basin. M.Sc. thesis. Tel Aviv Univ.(in Hebrew).

Guttman, J., 1998. Annual Report-1997.Sub project B: Hydrogeology of the eastern aquifer in the Judea Hills and Jordan Valley. Tahal. 6440-R98.006.

Guttman, J., Rosenthal A., 1991. Mitzpe Yericho area-Study of salinization mechanisms and water potential. Tahal Consulting Eng. Ltd. Rep.01/91/46 (in Hebrew).

Kafri, U., 1982. Relationship between the Dead Sea and groundwater levels in the western Dead Sea catchment area. Isr. Geol Surv. Current Res. 1981,90-94.

Kafri, U., 1984. Current subsurface seawater intrusion and migration of the groundwater divide in regions of tectonic instability in Israel. Geol. Soc. Am. Bull. 89, 223-227.

Kafri, U., Arad, A., 1978. Paleohydrology and migration of the groundwater divide in regions of tectonic instability in Israel. Geol. Soc. Am. Bull. 89, 1723-1732.

Kafri, U. Kessler, A., 2001. A program for hydrological planning for development of exploitation in the Kabri basin. Isr. Geol. Surv. Rep. GSI/36/01 (in Hebrew).

Kafri, U., Goldman, M., Lang B., 1997. Detection of subsurface brine, fresh water bodies and the interface configuration in between by the TDEM method in the Dead Sea Rift, Israel. Environ. Geol. 31, 42-49.

Kafri, U., Goldman, M., 2005. The use of the time domain electromagnetic (TDEM) method to delineate saline groundwater in granular and carbonate aquifers and to evaluate their porosity. J. Appl. Geophys. 57, 167-178.

Katz, A., Kolodny, Y., Nissenbaum, A., 1977. The geochemical evolution of the Pleistocene Lake Lisan-Dead Sea system. Geochim. Cosmochim. Acta 41, 1609-1626.

Kiro, Y., Yechieli, Y., Lyakhovsky, V., Shalev, E. and Starinsky, A., 2008. Time response of the water table and saltwater transition zone to a base level drop. Water Res. Res. doi:10.1029/2007WR006752.

Kronfeld, J., Vogel, J.C., Rosenthal, A., 1990. Natural isotopes and water stratification in the Judea Group Aquifer (Judean Desert), Israel. Isr. J. Earth Sci. 39, 71-76.

Laronne Ben-Itzhak, L., Gvirtzman, H., 2005. Groundwater flow along and across structural folding: an example from the Judean Desert, Israel. J. Hydrol. 312, 51-69.

Lensky, N., Dvorkin, Y., Lyakhovsky, V., Gertman, I. and Gavrieli, I., 2005. Water, salt, and energy balance of the Dead Sea. Water Res. Res. 41, doi:10.1029/2005WR004084.

Loetz, O.J., Ivelan, B., Robinson J.H. and Olms'tead, F.H. 1975. Geohydrology reconnaissance of the Imperial Valley, California. US Geol. Surv. Prof. Paper 486-K.

Matmon, D., 1995. Simulations of groundwater flow between the Mediterranean Sea and the Jordan rift valley, M.Sc. thesis, Hebrew Univ., Jerusalem.

McGarry, S., Bar-Matthews, M., Matthews, A., Vaks, A., Schilman, B. Ayalon,A., 2004. Constrains on hydrological and paleo-temperature variations in the eastern Mediterranean region in the last 140 ka given by the D values of speleothem fluid inclusions. Quat. Sci. Rev. 23, 919-934.

Oude Essink, G.H.P., 2001. Saltwater intrusion in a three dimensional groundwater system in the Netherland: A numerical study. Transport in Porous Media 43, 137-158

Rogers, D.B., Driess, S.J., 1995. Saline groundwater in Mini Basin, California. 2. Long term control of lake salinity by groundwater. Water Res. Res. 31(12), 3151-3169.

Salameh, E., El-Naser, H., 1999. Does the actual drop in Dead Sea level reflect the development of water sources within its drainage basin? Acta Hydrochim. Hydrobiol. 27, 5-11.

Sherif, M.M., Singh, V.P., 1999. Effect of climate change on sea water intrusion in coastal aquifers, Hydrol. Proc.13, 1277–1287.

Thiele, J., Gramann, F. and Kleinsorge, H. 1970. Zur Geologie zwischen dem Nordrand der ostlichen Kattara-Senke und der Mittelmeer-Kueste (Aegypten, westliche Wueste). Geol. Jb. 88, 321-354.

Tyagi, A.K., 2005. Impact of Sea Level Rise on Saltwater Intrusion in Coastal Aquifers, In: Raymond Walton, P.E. (ed.), Proceed.2005 World Water and Environ. Res. Congr., Anchorage, Alaska.

Yechieli, Y., 2000. Fresh-saline water interface in the western Dead Sea area. Groundwater 38, 615-623.

Yechieli, Y., 2006. The response of the groundwater system to changes in the Dead Sea level. In: Enzel, Y, Agnon, A., Stein, M. (eds.), New Frontiers in Dead Sea Paleoenvironmental Research, Geol. Soc. Am., Spec. Paper, pp. 241-253.

Yechieli, Y., Ronen, D., Berkovitz, B., Dershovitz, W.S., Hadad, A., 1995. Aquifer characteristics derived from the interaction between water levels of a terminal lake (Dead Sea) and an adjacent aquifer. Water Res. Res.31(4), 893-902.

Yechieli, Y., Gavrieli, I., Ronen, D., Berkovitz, B., 1998. Will the Dead Sea die? Geology 26(8), 755-758

Yechieli, Y., Kafri, U., Goldman, M., Voss, C.I., 2001. Factors controlling the configuration of the fresh-saline water interface in the Dead Sea coastal aquifers: synthesis of TDEM surveys and numerical groundwater modeling. Hydrogeol. J. 9, 367-377.

Yechieli, Y., Kafri, U., Wollman, S., Lyakhovsky, V., Weinberger, R., 2007. On the relation between steep monoclinal flexure zones and steep hydraulic gradients. Ground Water 45, 616-626.

Table 1. Hydrological parameters from pumping wells in the study area

Number	Borehole name	Coordinates	Sub-aquifer	elevation water level m, asl	T m2/day	Saturated thickness m	K m/day	Thickness of overlying S+E m	Amount of confinement m	Yield Q m3/h	Drawdown s m	Q/s	Remarks
1	En Karem 1	164909/131912	L	472	1100-3480	228	4.8-15.3			168	78	2.15	
2	En Karem 2	166032/133633	L	487		332				17	100	0.17	
3	En Karem 3	16207/13414	L	479		179				100	46	2.2	
4	En Karem 4	164161/131174	L	449		161				96	76.5	1.25	
5	En Karem 5	161465/133790	L	475		182				9	182	0.05	
6	En Karem 6	16226/13006	L	429	137-580	112	1.2-5			92	64.5	1.4	
7	En Karem 7	16160/13166	L	406		90							no water
8	En Karem 8	15902/13372	L	342<		0							no water
9	En Karem 9	166413/134754	L	488	4500-5560	162	31						
10	En Karem 10	167223/134656	L	485		446				101	61.9	1.63	
11	En Karem 11	163080/130854	L	454		135				8	83	0.1	
12	En Karem 12	169099/134556	L	488	9	385	0.03			48	96.5	0.5	
13	En Karem 13	16470/12790	L	447	248	210	1.2			186	113.8	1.63	
14	En Karem 14	16628/13400	L	481		175				318	92	3.4	
15	En Karem 15	165517/132822	L	480	7.9-16	200	0.04-0.08			85	50.2	1.7	
16	En Karem 16	166847/128048	L	450		277				252	94.7	2.7	
17	En Karem 17	167715/127775	L	448		300				80	55.4	1.44	
18	En Karem 18	164362/127123	L	458		179				320	4.1	78.5	
19	Jerusalem 1	168799/129495	L	480	22-53	388	0.06-0.14			204	101	2.02	
20	Jerusalem 2	169802/128778	L	580		92				11	87.5	0.12	
21	Jerusalem 3	169802/128778	L	438	18-30	480	0.03-0.06			48	79	0.6	
22	Jerusalem 4	1717/1307	L	484	32-110								
23	Jerusalem 5	17290/13270	L	358	46-90	385	0.12-0.23			19	19	1	
24	Jerusalem 6	17217/12559	L	233	960	470	2			151	52.7	2.8	
25	Jerusalem 11	17411/13876	L	128	63	311	0.2			64	62	1.03	
26	Shdema 1	172732/123053	L	212	200-280	427	0.5	100		15	20	0.75	
27	Shdema 2	17274/12306	U	202	315-357	89	3.54-4.01	114		25.5	4.2	5.95	acidification
28	Mukhmas	1748/1421	L	290		350				8	82.4	0.1	
29	El Azariya	17660/13200	L+U	48		300		50		169	57.03	2.96	
30	Herodion 1	170887/118263	U	353	96,291	122	0.79-2.38			42	48	0.87	
31	Herodion 2	170918/119328	L+U	341	580	520	1			288	38.8	7.4	
32	Herodion 3	1709/1175	L	294	216,296	358	0.6-0.83			206	78.3	2.6	
33	Herodion 4	16946/11408	L	360	93	230	0.4			40	78.8	0.51	acidification
34	Herodion 5	16946/11408	U	473	129	125	1			125	33.6	3.72	acidification
35	M Edomim 2	18270/13805	U	-154									
36	Miz. Yericho 1	1881/1352	L	-333									
37	Miz. Yericho 2	18825/13434	L	-341	5000	170	30	48		302	11.7	25.8	acidification
38	Miz. Yericho 5	18820/13770	L	-348	>20000	90		150		314	4.76	66	
39	Miz. Yericho 6	189122/138505	L	-339	211	105	2	39		114	58.2	1.95	
40	Yericho 1	19090/14080	L	-324	1180-1280	99	11.9-12.9			245	26.8	9.14	
41	Yericho 2	190718/139482	L	-330	1350	430	3.1	60		330	36	9.2	
42	Yericho 4	1894/1452	L	-305	126-380	428	0.3-0.9			112	145.7	0.8	acidification

43	Yericho 5	18825/14685	L	-306	150-305	390	0.4-0.8	105		102	69.95	1.71	acidification
44	Modiin 2	154286/139791	L+U	16		790		165		235	2.84	82.7	appar. thickness
45	Modiin 3	153070/137146	L	16		616		195		450	13.75	32.7	appar. Thickness
46	Modiin 4	153588/138651	L	10	2072	440	4.7	288	55	580	14.4	40.2	
47	Eshtaol 1	15113/13164	U	21		150		325	95	204	3.17	64.4	
48	Eshtaol 2a	151350/131650	U	17	155	300	0.5	260	30				
49	Eshtaol 3	15234/13594	U	19		152		140		248	3	82.7	
50	Eshtaol 4	151302/134141	U	18		288		290	12	346	1.05	330	
51	Eshtaol 5	152574/131662	L	24	5450	240	23	0		200	42.9	4.66	acidification
52	Eshtaol 6	151591/135275	L	21		251		279	8	495	46	10.3	
53	Eshtaol 7	151525/130604	L	24	700	430	1.6	400	157	576	46.25	12.45	acidification
54	Eshtaol 8	151990/134480	L	24	9600-28000	420	22.8-67	0		443	3.53	125.5	
55	Eshtaol 9	151680/133001	L	20		400				510	9.97	51.2	
56	Hartuv 3	150963/129813	U	22	500	145	3.4	375	172	108	11.59	9.35	
57	Ajur 6	150970/120846	U	20				270		126	28.85	4.36	
58	Ajur 7	15220/12070	L	30	20350	300	68	0		600	8.95	67	
59	Ajur 8	15150/12440	L	25		400				545	8.02	67.9	appar. Thickness
60	Ajur 10	151860/122312	L	22		550		24		275	22.8	12	appar. thickness
61	Achisemach 1	14240/14980	L	16	11842	220	54	65	28	942	3.61	215.1	
62	Achisemach 2	141929/149770	L	12		530		70		508	33.83	15	
63	Gimzu 1	144974/149275	U	13		43				300	0.1	3000	
64	Gimzu 1 deep	144974/149275	L	16		?				312	62.6	4.98	
65	Yarkon E 3	142140/149825	U	39		105		78	37	360	0.38	950	
66	E. Ayalon 1	14320/14570	U	30		38		0		192	1.15	167	
67	Ayalon 2	14416/14516	U	25	54000	400	135	20		147	0.18	816	
68	Ayalon 3	14535/14212	U	25		54		292	189	240	2.44	98	
69	Ayalon 4	14473/14478	U	41		41		0		178	0	9999	infinite Q/s
70	Ayalon 5	143722/144608	U	24				45		240	0	9999	infinite Q/s
71	K. Uriya 3	14610/13420	U	24		200+		130		356	6.71	53	
72	K. Uriya 4	14238/13597	U	23		15		55		312	0	9999	infinite Q/s
73	K. Uriya 5	14325/13575	U	25		41		70		210	0	9999	infinite Q/s
74	K. Uriya 6	145304/134391	U	24		119		140		300	0	9999	infinite Q/s
75	K. Uriya 7	14673/13001	U		4000	300	13	300					
76	K. Uriya 8	14470/13700	U	25		56		86		355	0.36	1000	
77	K. Uriya 10	142908/135541	U	14		136		45		382	51.85	5.4	
78	T. Zafit 1	136956/123849	U	15		?		300	180	576	1.89	304.8	
79	Ajur 2	14198/12580	U	24		58		517	330	330	13	25.3	
80	Ajur 4	148234/121389	U	16		250		525	265	330	4	82.5	
81	Ajur 5	149097/120851	U	17	141	150	0.94	540	271	192	67.3	2.85	
82	K. Menachem 1	13220/12750	U	28		438		345	293	270	15.1	17.9	
83	Nechusha 1a	137473/115464	U	17	2400	200	12	628	435	720	65.28	11.03	
84	Zoharim 1	144862/113484	U	10		150		700	400	400	5.9	67.8	

Table 2. Groundwater flow rates to the Mediterranean Sea and the Dead Sea

Scenario	Transient / Steady-state	Total Recharge (mcm/yr/km)*	Western base level (m)	Eastern base level (m)	Flow to the Dead Sea (mcm/yr/km) *	Flow to the Mediterranean (mcm/yr/km) *
Present day (1960)	SS	4.9	+10	-395	2.6	2.3
Future (1000 yr) - following Dead Sea level decline	Trans	4.9	+10	-395 to -545	2.7	2.2
Lisan Lake Period (same recharge as today)	SS	4.9	-120	-180	2.5	2.4
Lisan Lake Period (150% of today's recharge)	SS	7.4	-120	-180	3.7	3.7

- \- values are given for a strip 1 km wide.

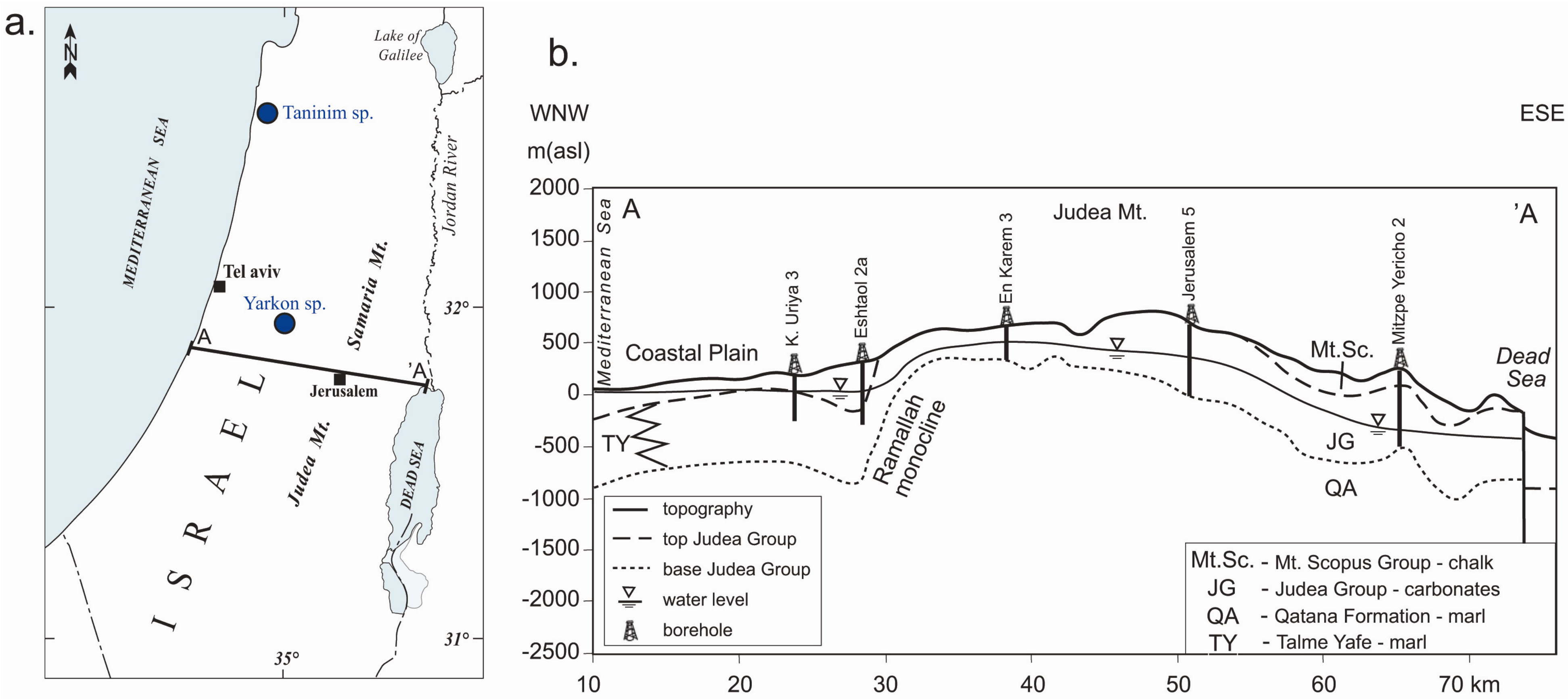

Figure 1: a. Location map of cross-section (A-A');

b. Simplified hydrogeological cross-section from the Mediterranean Sea to the Dead Sea.

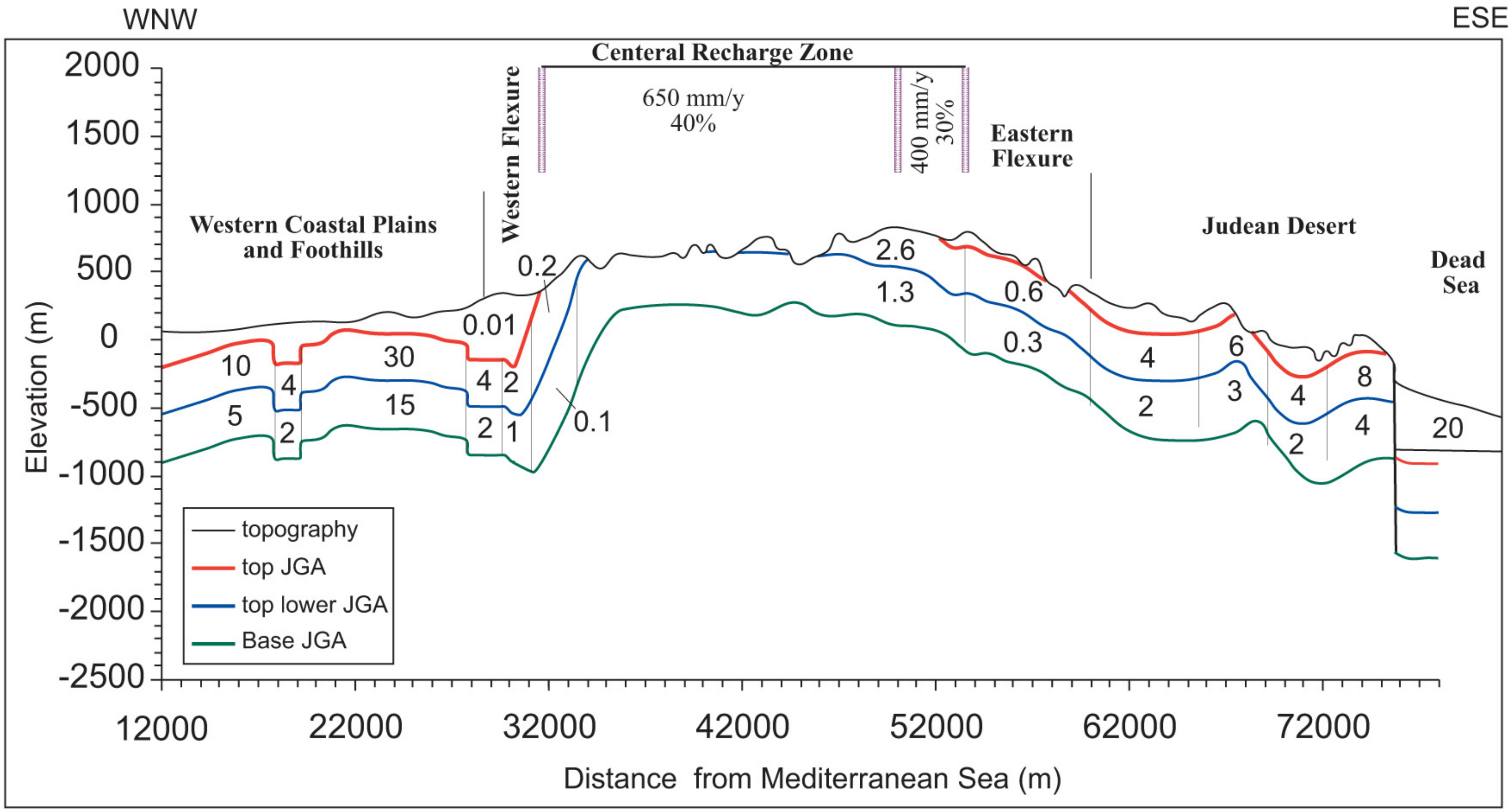

Figure 2: Calibrated values of horizontal hydraulic conductivity (m/d) and recharge in the JGA.

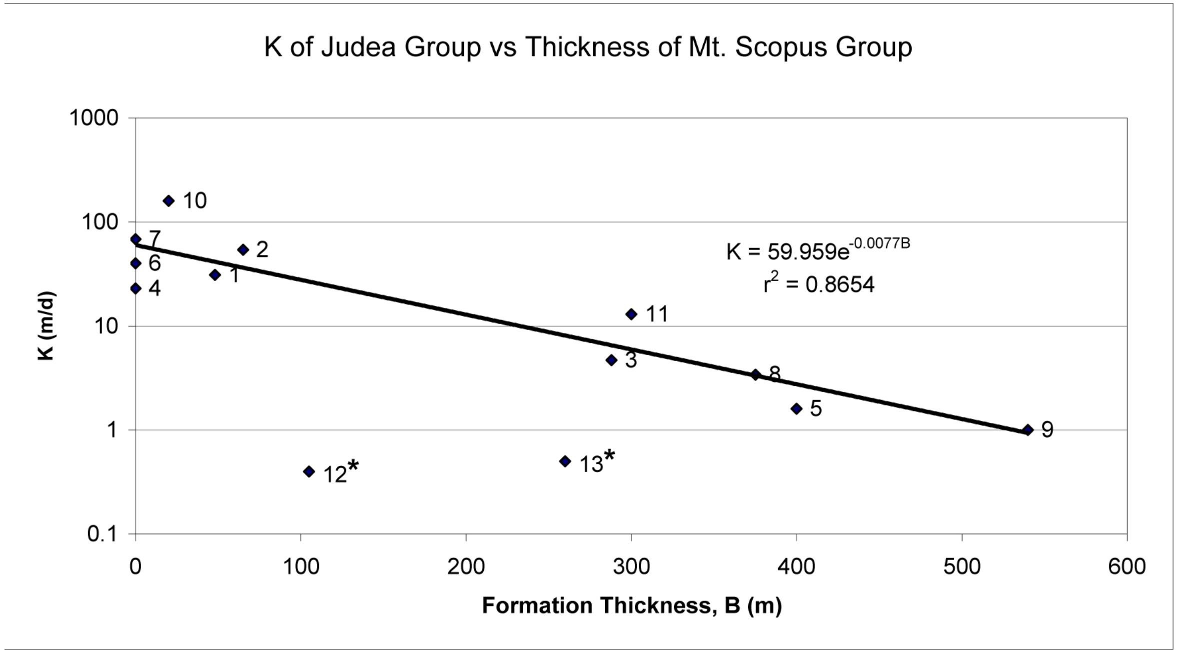

No.	Borehole Name	Formation thickness, B (m)	K (m/d)
1	Mitzpe Yericho 2	48	31
2	Achisemach 1	65	54
3	Modiin 4	288	4.7
4	Eshtaol 5	0	23
5	Eshtaol 7	400	1.6
6	Eshtaol 8	0	40
7	Ajur 7	0	68
8	Hartuv 3	375	3.4
9	Ajur 5	540	1
10	Ayalon 2	20	160
11	Kefar Uriya 7	300	13
12*	Yericho 5	105	0.4
13*	Eshtaol 2a	260	0.5

* not included in regression analysis

Figure 3: K vs thickness of the overlying Mt. Scopus Group.

* Eshtaol 2a and Yericho 5 boreholes are exceptional and excluded for the following reasons: Eshtaol 2a has a low K value related to its local condition within the flexure zone (Yechieli et al., 2007) ; Yericho 5 probably abuts a major fault and exhibited considerable drawdown in the course of a pumping test due to its low transmissivity and K values.

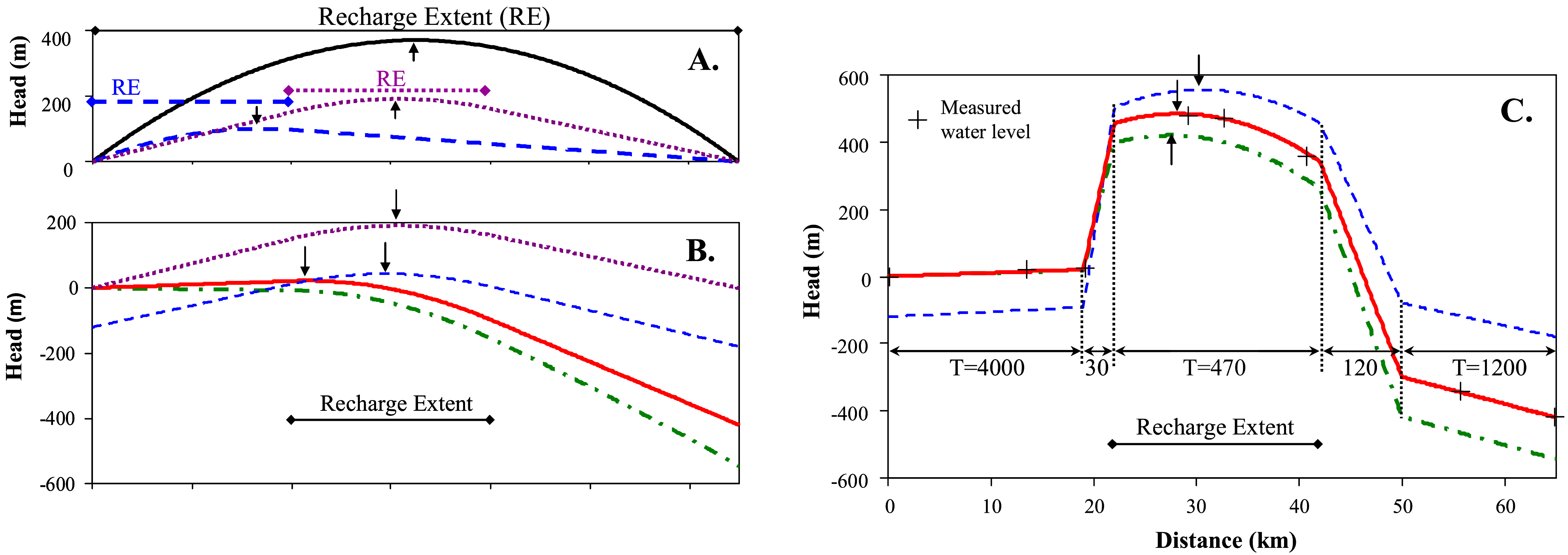

Figure 4: Examination of the structural effect on the location and elevation of the groundwater divide, using 1-D analytical solution, conducted with Mathcad software. Arrows denote the location of the water divide. Recharge was taken as 250 mm/year in all cases.

a. Effect of the location of the recharge (uniform transmisivity; T=1000 m^2/day). The colors denote different extents of the recharge

b. Effect of elevation of base levels (uniform transmisivity; T=1000 m^2/day). The different colors denote different base levels.

c. Effect of elevation of base levels with non-uniform transmissivity. The different colors denote different base levels (same as in Fig 4b).

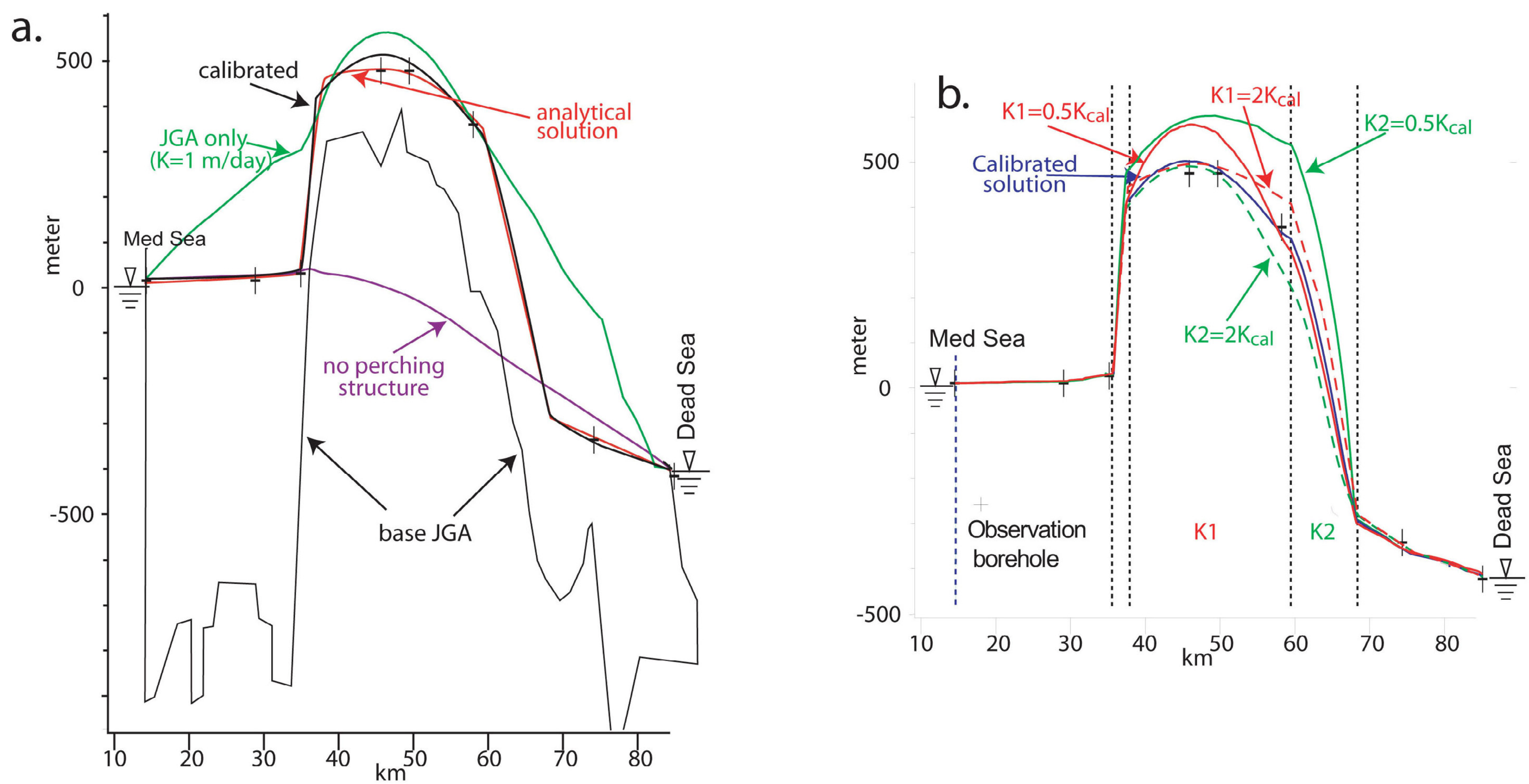

Figure 5: Simulations of different hydrogeological parameters, using the FEFLOW code.

a. Two basic configurations are exhibited: A structural controlled impermeable boundary at the base of JGA and a case without such a boundary.

- Red line – analytical solution, lateral segmentation of K.
- Black line – calibrated FEFLOW simulation with an impermeable boundary at the base of JGA.
- Green line – FEFLOW simulation with homogeneous lateral K distribution and impermeable boundary at the base of JGA.
- Purple line – homogeneous lateral K distribution with a bottom impermeable boundary considerably below the base of JGA (1000 m), with no significant effect of geometry.

For all cases, recharge distribution is as given in Figure 2.

b. Effect of variations in the hydraulic conductivity in the different parts of the aquifer.

a.

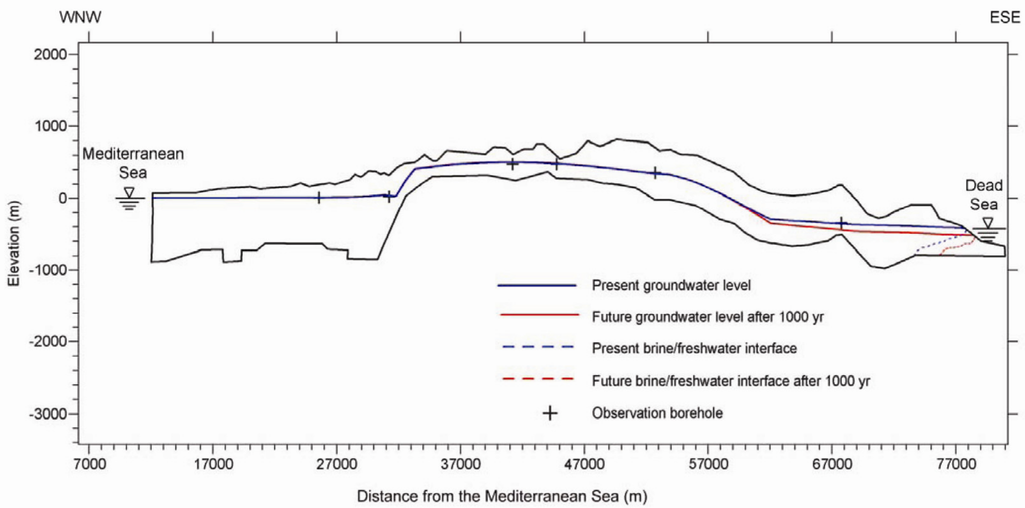

b.

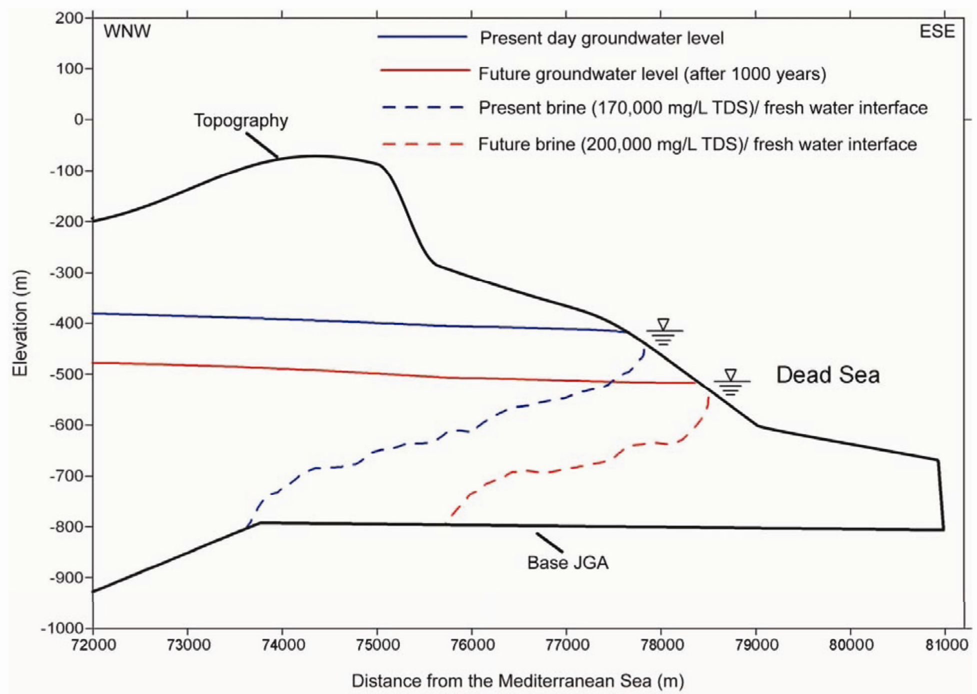

Figure 6: a. Present groundwater level and simulated future ones, after 1000 years.

b. A close-up of the simulated brine/freshwater interface configuration near the Dead Sea, at present and after 1000 years. The isochlors represent the present-day salinity (170 g/l) and the future salinity (200 g/l).

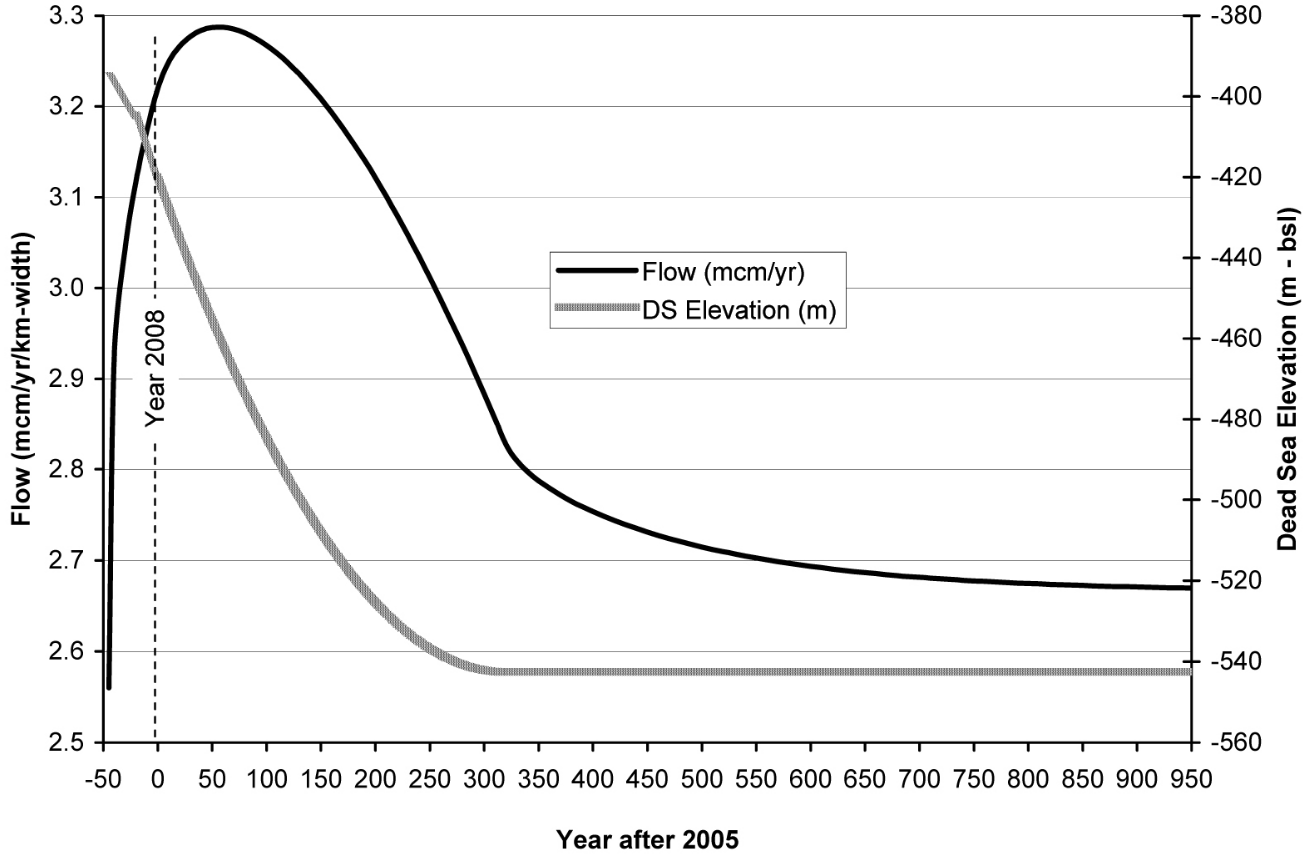

Figure 7: a. Estimated future drop in the Dead Sea level (modified after Yechieli et al., 1998).

b. Simulated groundwater flow to the Dead Sea due to the future declining lake level. The drop in groundwater discharge to the DS follows the change in the rate of the DS level drop.

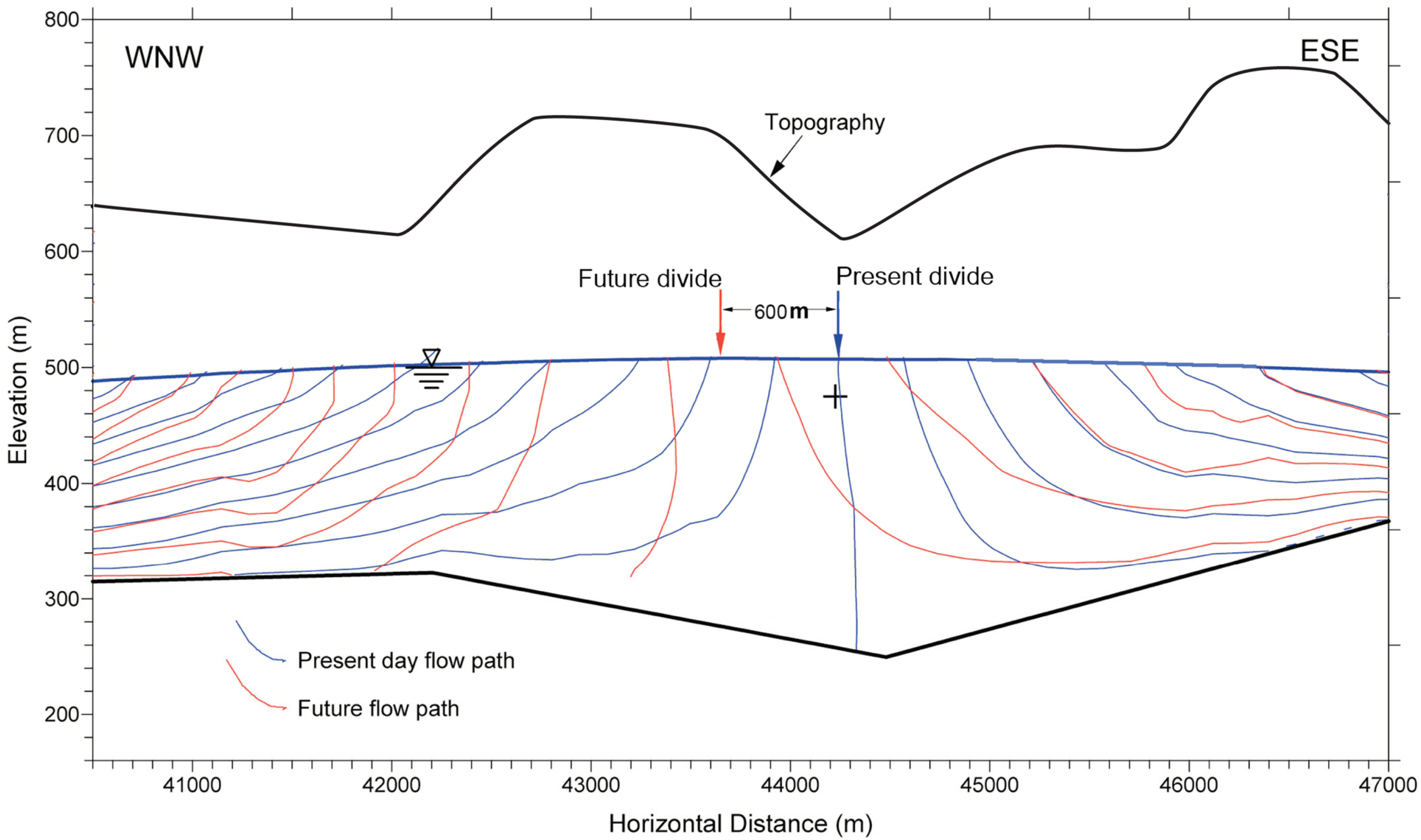

Figure 8: Flow paths showing the shift of the groundwater divide due to the future Dead Sea level decline. Note that the scale here is larger than in Figures 5a and 6.

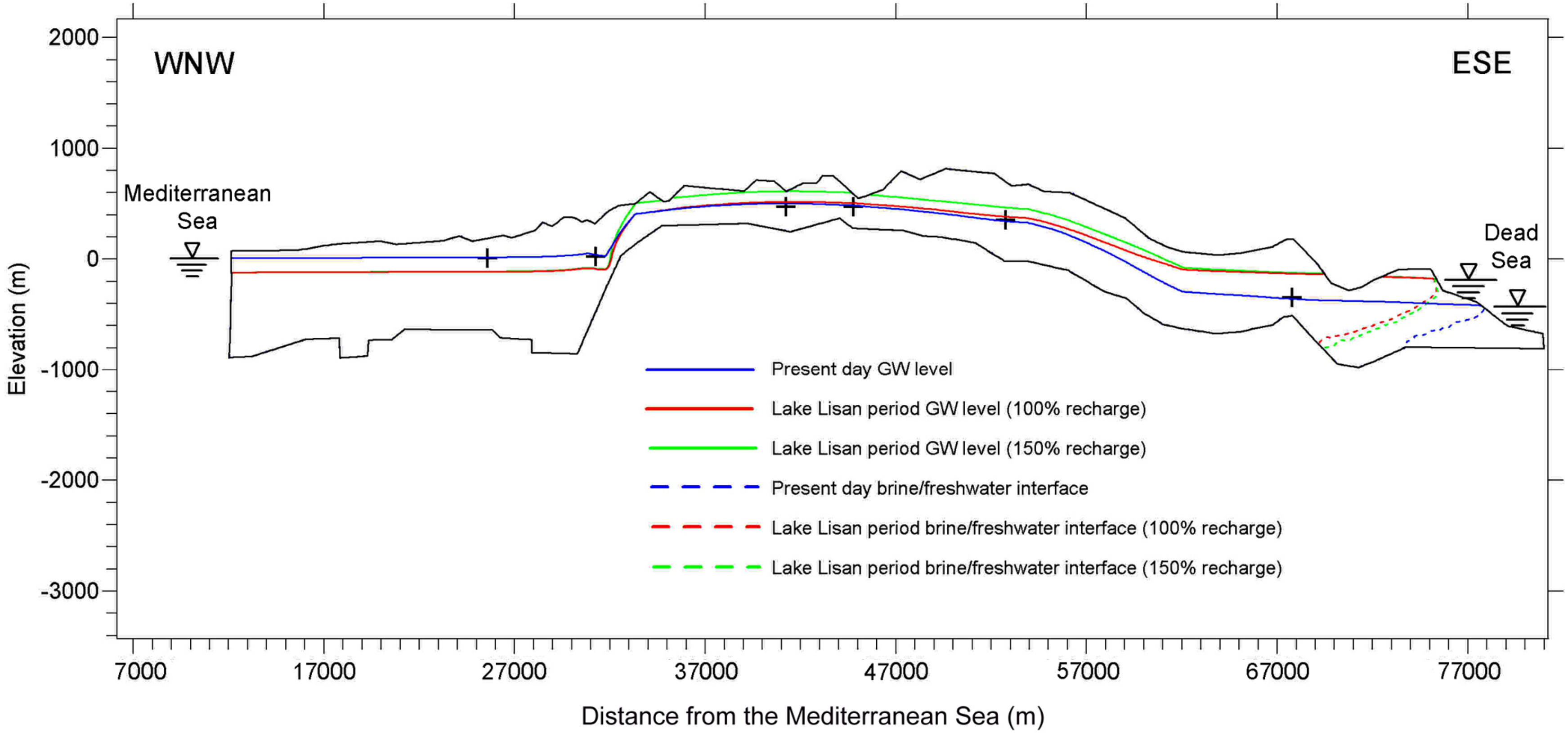

Figure 9: Simulation results of the Lake Lisan period (100% and 150% recharge scenarios) as compared with the present situation.